PAPER

Optical states in a 1D superlattice with multiple photonic crystal interfaces

IOP Publishing Journal of Optics
J. Opt. **22** (2020) 065101 (9pp) https://doi.org/10.1088/2040-8986/ab896c

Optical states in a 1D superlattice with multiple photonic crystal interfaces

Nicholas J Bianchi and Leonard M Kahn

University of Rhode Island, Kingston, RI, United States of America

E-mail: lenkahn@uri.edu and nicholasbianchi@uri.edu

Received 8 January 2020, revised 20 March 2020
Accepted for publication 15 April 2020
Published 19 May 2020

Abstract

Interface states in a 1D photonic crystal heterostructure with multiple interfaces are examined. The heterostructure is a periodic network consisting of two different photonic crystals. In addition, the two crystals themselves are periodic, with one being made of alternating binary layers and the other being a quaternary crystal with a tunable layer. The second crystal can thus be smoothly transformed from one binary crystal to another. All individual photonic crystals in the superstructure have symmetric unit cells, as well as identical periods and optical path lengths. Therefore, as the tunable layer in the quaternary crystal expands, other layers will shrink. It is found that the behavior of the localized modes in the band gaps is dependent on whether there is an even or odd number of interfaces in the heterostructure. With certain sequences of all dielectric photonic crystals, topological states are shown to split in two, whereas for other heterostructures they are shown to vanish. Additional resonant Tamm states appear depending on how many crystals are in the heterostructure. If the tunable layer is frequency dependent, the band gap can still support topological/resonant modes with some band gaps even supporting two separate groups.

Keywords: interface state, heterostructure, photonic crystal

1. Introduction

A photonic crystal (PC) is a periodic array of dielectrics and/or conductors used to scatter light [1, 2]. In a similar manner to how semiconductors control the passage of electrons, PCs possess passbands, which allow photons in certain frequency ranges to propagate through the crystal, and photonic band gaps (PBGs), which inhibit photon flow, producing regions of suppressed transmission. The existence of these pass and stop bands are governed by Bloch's thereom. Photonic heterostructure devices are comprised of multiple periodic components that can produce transmission properties and field localization not seen in isolated crystals [3, 4]. Heterostructures consisting of two PCs with a shared interface have been extensively studied. This interface can support localized modes known as optical Tamm [5] states (OTSs) if electromagnetic field amplitudes decay away as the distance from the boundary increases in either direction. This means the wavevectors in both directions must be imaginary. In the case of a PC, this occurs if the mode is trying to travel through a PBG. These modes have been found in a variety of photonic structures [6–12]. Tamm states have also been investigated in systems containing a PC with a tunable cap layer adjacent to a uniform medium. Examples include PCs containing superconducting layers [13], systems containing metamaterials, both the PC layers [14, 15] and the uniform medium [16], and systems with liquid crystal [17] and chiral [18] cap layers. In addition, OTSs have also been studied at a metal/PC interface [19–21].

If an interface is generated between two PCs with symmetric unit cells, Tamm states at the boundary can form that are governed by the bulk band structure of the two crystals. These states are referred to as topological interface states. Xiao *et al* [22] showed that their existence in a PBG can be predicted by ensuring that the imaginary parts of the surface impedances for the two crystals sum to zero in the selected gap. Their work established a relation between the sign of the impedance, Z, for a PBG and the sum of all Zak [1] phases, θ_m^{zak}, below the gap, where m denote the (isolated) bands,

$$\mathrm{sign}(\mathrm{Im}(Z^{(n)})) = (-1)^{n+l}\exp\left(i\sum_{m=0}^{n-1}\theta_m^{zak}\right) \qquad (1)$$

In equation (1), n is the PBG where the impedance is calculated and l denotes the number of points where two bands cross below band gap n. Due to the PC unit cells possessing inversion symmetry, all Zak phases can only take on the values of π or 0 [1], and thus provide a useful measure for identifying topological states. Band gap n contains a topological state if $\mathrm{Im}(Z_L + Z_R) = 0$, where the subscripts indicate the PCs to the left/right of the interface. Through control of θ_m^{zak}, topological states have been demonstrated in both 1D [24, 25] and 2D [26] systems.

The behavior of PBGs in inversion symmetric quaternary photonic crystals was first described in [27–29]. While multiple states, including topological, plasmons, etc, have been studied in multi-crystal heterostuctures, they usually require both a conducting layer and either a thin Kerr medium [30] or graphene monolayer [31–33] be inserted among the two Bragg gratings (PCs). To the best of our knowledge, no attempt has been made to generate interface states in a purely dielectric binary/quaternary heterostructure consisting of multiple PCs. Ternary PCs are not considered here since their unit cells cannot be made inversion symmetric, which is needed to produce topological states [22]. Ensuring the unit cells are inversion symmetric also allows us to exhange the order of two PCs across a single interface without any change in transmission. In our previous manuscript [34], we extended Xiao's work to a system with one binary PC and one quaternary PC, containing a tunable layer (layer C in figure 1). The behavior of topological states in this structure was studied. The goal of this manuscript is to extend the work in our previous paper by creating a heterostructure of alternating binary and quaternary crystals. Now there is an overall periodicity in the order of the individual crystals, in addition to the material periodicity in the crystals themselves (see figure 1). This multi-binary/quaternary structure is advantageous, compared with the multi-binary/binary heterostructure, as we can not only generate transmission bands composed of multiple OTSs within a PBG [35], but also finely tune their frequencies through the use of the additional layer. In addition, Chen's [35] transmission bands possess a noticeable gap in the middle. We show that if one of the crystals at the ends of the heterostructure is quaternary while the other is binary, the topological state coexists with the OTSs. We also find that if both the first and last PCs are quaternary, the topological state splits in two during the topological phase transition, as the tunable layer grows. In section 3, we also discuss what happens if the tunable layer is frequency dependent via the Drude model [36]. To possess the split topological state with the metallic layer, the configuration must be sandwiched by the binary PCs, rather than by quaternary PCs. Table 1 summarizes the advantages and disadvantages of various interfaces.

2. Methods

Our work was conducted using the transfer matrix method (TMM) [37]. Keeping with [34], all variables are made dimensionless for convenience. The lengths of the individual PC layers, l_i, are scaled to the unit cell period, Λ: $d_i = l_i/\Lambda$ and are

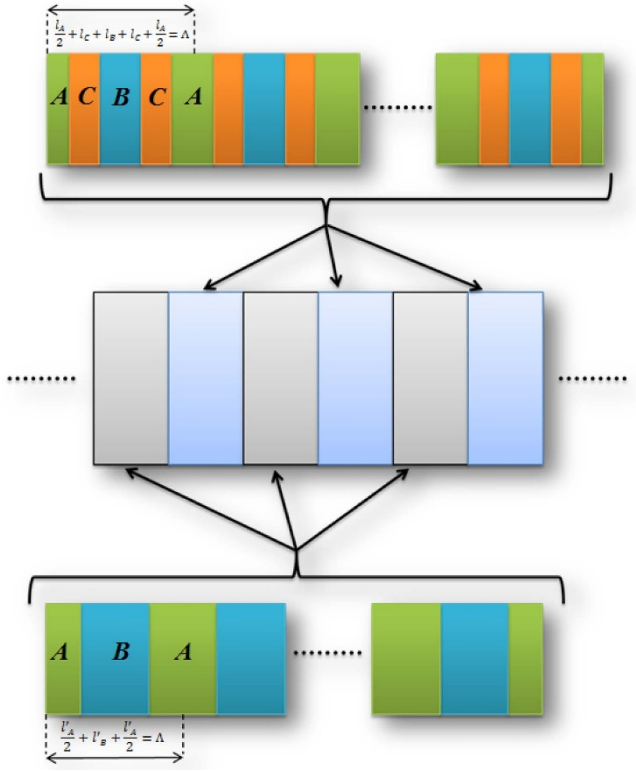

Figure 1. Schematic of PCs and overall heterostructure. The heterostructure is displayed in the middle as repeating light grey and blue 'slabs'. Each of these 'slabs' represent entire photonic crystals. The grey slabs represent binary PCs, displayed at the bottom. In the bottom diagram, dark green is layer A and dark blue is layer B. The vertical dashed lines and double arrow show one unit cell. The primes indicate that the individual layer lengths are different from those of the quaternary PC. Note that the PC is capped on both sides with a half-width of layer A, making the unit cells symmetric. The top diagram shows the quaternary PC, which is represented in the middle picture as the light blue regions. In the quaternary PC, layers A and B are the same material as in the binary crystal. Layer C is orange. As in the binary case, the symmetric unit cell is displayed by the double arrow.

such that Λ and the optical path, Γ, for a unit cell are constant. In the heterostructure, shown as the middle image in figure 1, the periods for all the individual PCs are equal, as are the optical paths. The binary PCs are the gray regions and the quaternary PCs are the light blue regions. Since there is no fixed length scale, we set $\gamma = \Gamma/\Lambda$. For the quaternary PC, shown at the top of figure 1, the widths of layers A, in green, and B, in blue, can be expressed in terms of a free parameter, the width of the introduced layer, d_C, in orange, [34],

$$d_A = \frac{\gamma - n_B - 2(n_C - n_B)d_C}{n_A - n_B} \tag{2}$$

$$d_B = \frac{\gamma - n_A - 2(n_C - n_A)d_C}{n_B - n_A}. \tag{3}$$

Quaternary PCs are useful because, by varying d_C, it is possible to change d_A and d_B while maintaining a constant optical

Table 1. Summary of various PC interfaces. *b* is binary PC and *q* quaternary PC. Both are assumed inversion symmetric. Last three rows are for this work

Types of interfaces		
Configurations	Advantages	Disadvantages
Air/PC [11]	(i) Single PC. (ii) Supports guided modes for oblique incidence. (iii) Surface cap layer can be used to make states.	(i) No Tamm states at normal incidence (without cap).
Metal/PC [19–21]	(i) Tamm plasmons possible for both TM and TE polarizations. (ii) Tamm plasmons possible both above and below plasma frequency.	(i) Loss can reduce transmission. (ii) Condition for existence dependent of whether formed above or below plasma frequency.
Metal/PC/metal [39]	(i) Useful for switching between Fabry-Perot resonances and Tamm states from low to high index layer contrast.	(i) Metal thickness less than skin depth produce ill-defined normal modes.
(General) PC/PC [6–9]	(i) Tamm states possible for both TM and TE polarizations. (ii) Lossless	(i) Both PCs must have overlapping PBGs
b/b [22, 24, 25]	(i) States described by bulk band topology.	(i) Limited tunable parameters (two indices, two thicknesses)
b/q [34]	(i) Using tunable third layer, possible to examine state behavior as PC transforms: binary - quaternary - new binary	(i) Topological phases cannot be found analytically.
b/b/b/.../b/b/b [35]	(i) OTSs in gap form transmission band.	(i) Topological states not present.
b/q/b/.../q/b/q	(i) Preserves topological state	(i) State transmission decreases with more layers.
b/q/b/.../b/q/b	(i) Tunable OTS transmission band	(i) No topological states for all dielectric case
q/b/q/.../q/b/q	(i) Split topological state for all dielectric case	(i) Increasing unit cells makes topological states harder to resolve.

path as well as all refractive indices. This is not possible for a binary PC. For a binary crystal, to change d_A and d_B, you must either change γ, n_A, or n_B. To fabricate these structures, it is much easier to tune a length (i.e. d_C), rather than a refractive index.

Note that d_C can only take on values in which both equations (2) and (3) are non-negative. When d_C reaches its maximum, the quaternary PC will become binary again, but with configuration, ...*CBCBC*..., if d_A tends to zero, or, ...*ACACA*..., if d_B tends to zero. For the special case, $\gamma = n_C$, both d_A and d_B will be zero when d_C reaches its maximum; this will result in a uniform layer *C*. The lengths of the layers in the binary PC, displayed at the bottom of figure 1, are simply equations (2) and (3) but with $d_C = 0$ and thus do not change. The index of refraction of layer j is $n_j^2 = \epsilon_j \mu_j$, where ε_j and μ_j are the (relative) permittivites and permeabilites. In the binary and quaternary crystals, the n_A's are the same and the n_B's are the same, although $n_A \neq n_B$ [34].

For the system described in figure 1, we only consider an electric field incident from the left, E_{1+}. The reflected field is E_{1-} and the field that is transmitted through the entire structure is $E'_{(N+1)+}$. To compute the transmission spectra for the system, first we must construct the transfer matrix, $\mathbf{M}$, from the individual interface matrices, $\mathbf{I}_j$, and propagation matrices, $\mathbf{P}_j$, where the index, j, specifies the layer in question [38],

$$\mathbf{I}_j = \frac{1}{\tau_j}\begin{pmatrix} 1 & r_j \\ r_j & 1 \end{pmatrix} \tag{4}$$

$$\mathbf{P}_j = \begin{pmatrix} e^{2\pi i n_j d_j \xi} & 0 \\ 0 & e^{-2\pi i n_j d_j \xi} \end{pmatrix} \tag{5}$$

where r_j and τ_j are the reflection and transmission coefficients, respectively,

$$r_j = \frac{\mu_{j+1} n_j - \mu_j n_{j+1}}{\mu_{j+1} n_j + \mu_j n_{j+1}} \tag{6}$$

$$\tau_j = \frac{2\mu_{j+1} n_j}{\mu_{j+1} n_j + \mu_j n_{j+1}}. \tag{7}$$

In scaled variables, the phase argument, $ik_j l_j$ becomes $2\pi i n_j d_j \xi$. The frequency, f, becomes $\xi = f\Lambda/c_0$, where c_0 is the speed of light in vacuum. The incident and scattered field are related by,

$$\begin{pmatrix} E_{1+} \\ E_{1-} \end{pmatrix} = \begin{pmatrix} M_{11} & M_{12} \\ M_{21} & M_{22} \end{pmatrix} \begin{pmatrix} E'_{(N+1)+} \\ 0 \end{pmatrix} \tag{8}$$

where,

$$\mathbf{M} = \begin{pmatrix} M_{11} & M_{12} \\ M_{21} & M_{22} \end{pmatrix} = \prod_{j=1}^{N} \mathbf{I}_j \mathbf{P}_j \mathbf{I}_{N+1}. \tag{9}$$

The transmitted power is calculated via,

$$T(\xi, d_C) = \left\| \frac{1}{M_{22}} \right\|^2 \tag{10}$$

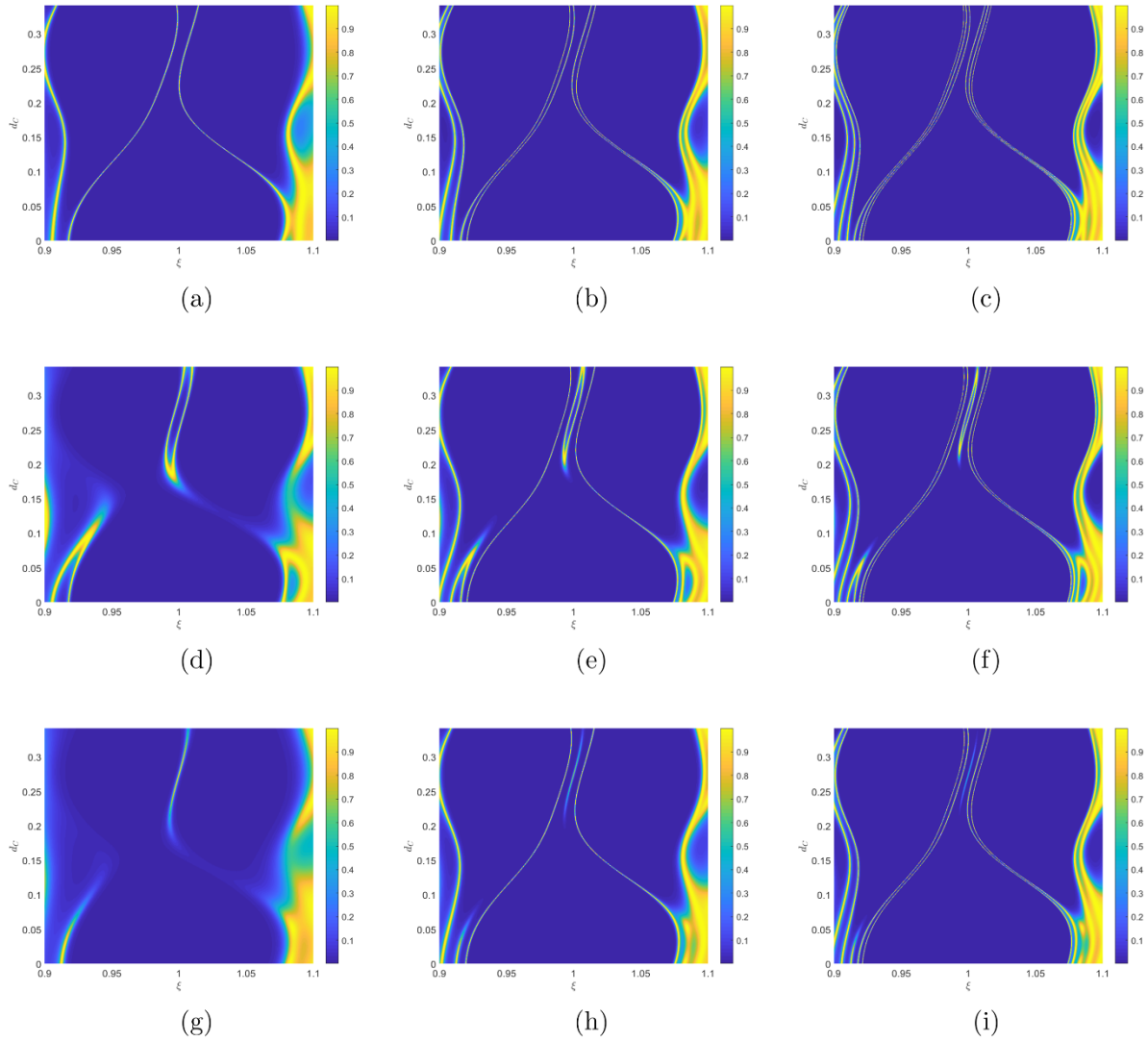

Figure 2. Transmission map for PC heterostructure in 3rd PBG. The stucture consists of alternating binary (b) and quaternary (q) PCs. Each PC has 4 symmetric unit cells. $\varepsilon_A = 6$, $\varepsilon_C = 3$, $\epsilon_B = \mu_A = \mu_B = \mu_C = 1$ (a) bqb, (b) $bqbqb$, (c) $bqbqbqb$, (d) qbq, (e) $qbqbq$, (f) $qbqbqbq$, (g) bq [34], (h) $bqbq$, (i) $bqbqbq$.

3. Results

In our first investigation, all layers of the heterostructures are assumed to be lossless dielectrics with no material dispersion. For both the binary and quaternary PCs, $\epsilon_A = 6, \epsilon_B = \mu_A = \mu_B = 1$. In the quaternary PC, $\varepsilon_C = 3$ and $\mu_C = 1$. For simplicity, all PCs are given the same number of unit cells,N_Λ, periods and optical paths. In the following systems, $N_\Lambda = 4$ and $\gamma = 1.5$. With d_C as a free parameter, d_A and d_B of the quaternary PC are described by equations (2) and (3). We restrict ourselves to the 3rd PBG. For convenience, when describing individual PCs of the heterostructures, we will use b for binary PC and q for quaternary PC [34].

Figure 2 displays nine different transmission examples, with the results summarized in table 2. In figures 2(a)–(c), the stucture is sandwiched between two binary PCs, while in figures 2(d)–(f), the two endlayers are quaternary PCs. In both cases, the number of interfaces between individual PCs from left to right is two, four and six. Since there is an even number of interfaces in the heterostructure, a single topological peak (figure 2(g)) is absent, even though equation (1) states that there is a change in the sign of surface impedance between the binary and quaternary components as d_C increases from 0 to 0.341. For the transmission maps in the top row, the

Table 2. Description of states present in figure 2.

Configuration	# of OTSs	Topological state
bqb	2	none
bqbqb	4	none
bqbqbqb	6	none
qbq	0	split
qbqbq	2	split
qbqbqbq	4	split
bq	0	single
bqbq	2	single
bqbqbq	4	single

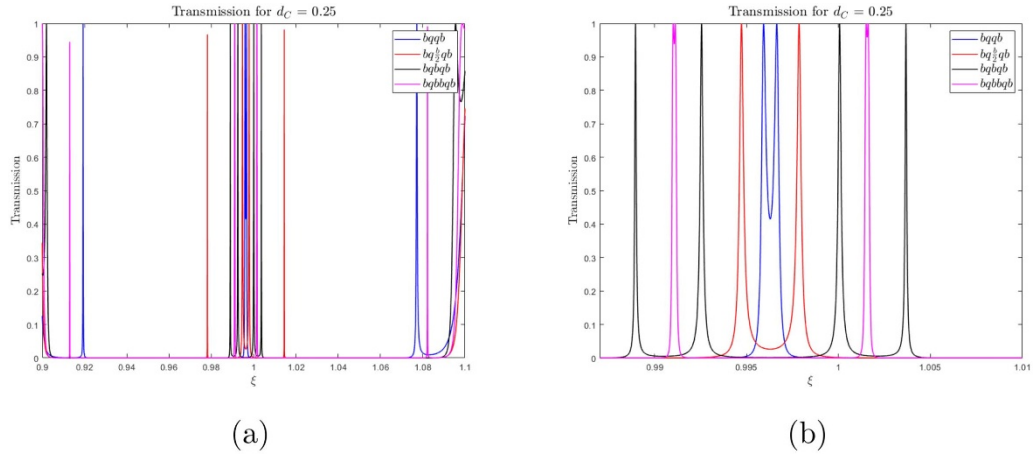

Figure 3. (a) Transmission resonance behavior for PC heterostucture *bq...qb* as the number of central binary crystals varies. Each *b* and *q* represents four unit cells (*b*/2 is two unit cells). (b) Central region of (a).

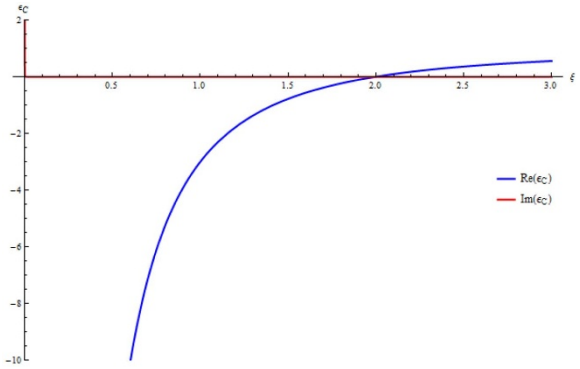

Figure 4. Real and imaginary parts of ε_C for metallic layer *C*. Plasma frequency $\xi_p = 2$ and collision frequency $g = 10^{-10}$. Frequencies are scaled according to $\xi = f\Lambda/c_0$.

heterostructure has the form *bqb*, *bqbqb* and *bqbqbqb*. It can be seen that the state in a single interface system splits into two sets of OTSs, with one set below the original frequency and the other above [35]. At $d_C = 0$, all these states exist as Fabry–Perot modes; however, as d_C increases, they begin to wander into the band gap, becoming Tamm-like. Transitions between Fabry–Perot and Tamm states have also been studied in PCs capped by metal layers [39]. As these Tamm states appear at all values of d_C, they are not topological in nature, although after the impedance for the quaternary layers flips sign (see equation (1)), they appear to cluster together in the region where the topological state in the single binary-quaternary interface heterostructure was located. The transmission for all these states remains at unity for all values of d_C. This transmission band of OTSs behaves differently from resonances caused by a sequence of defect modes [40], which are evenly spaced with no central gap in the transmission band.

When the heterostructure changes from *bqb* to *bqbqb*, the two states themselves split into pairs [35] such that these pairs (figure 2(b)) each have a higher and lower frequency state relative to their respective states in figure 2(a). This splitting is illustrated in figure 3. A horizontal slice of figure 2(b) at $d_C = 0.25$ is considered, except now the states are plotted for varying thickness of the middle cystral. Each binary and quaternary represent four unit cells; *b*/2 represents two unit cells. In figure 3(a), we see two distant edge states (blue) in the absence of a middle *b*: *bqqb*. To see the two interface states, though, we must zoom into the cluttered middle region. These interface states are clearly seen in figure 3(b). When two binary unit cells are inserted in the center of the structure (*bq*(*b*/2)*qb*), there is now strong coupling between the two central states and the two edge states. The edge states rapidly move toward the central region. Inserting another two binary unit cells produces the familiar structure *bqbqb* and the black transmission profile. Doubling the central region causes coupling of the states in each pair to weaken due to the increased distance [32, 33] between the interface pairs *bqb*. This is seen in the magenta curve as the four peaks mostly merge into two, recovering figure 2(a) at $d_C = 0.25$. There is also a new pair of edge states in figure 3(a).

An important change occurs in the transmission behavior as d_C increases if the sandwiching layers are quaternary. In figure 2(d), the heterostructure is *qbq* and a topological state is observed in the upper half of the map; however, it splits into two separate peaks since there are two interfaces. With additional layers, the structure becomes *qbqbq* and *qbqbqbq*, shown in figures 2(e) and (f) respectively. Here the split topological state is surrounded by resonant states that behave similarily to those described in figure 3 [35]. To help understand why the topological state appears in the *qb...bq* but not the *bq...qb* configuration, it is helpful to examine the behavior of the band at small d_C. Recall that when equation (1) produces opposite signs for the isolated quaternary and binary PCs, the number of resonant states in the middle of the PBG must be equal to the number of interfaces in the composite heterostructure. For *bq...qb*, all the states remain separate (i.e. states do not merge). For example, let us consider figure 2(c). Since there are six interfaces, the six states that enter the band gap are the three closest pass band states on either side of the gap. Compare this to figure 2(f), where only the two closest states on either side of the PBG wander into the gap when d_C increases

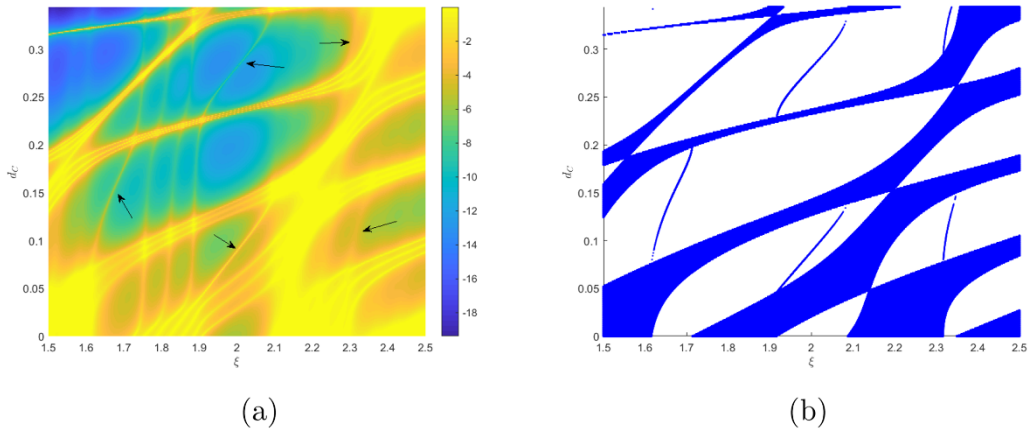

Figure 5. (a) Transmission map behavior for PC heterostucture *bq* where the quaternary PC contain metallic layer *C*. $\varepsilon_A = 6$, $\epsilon_B = \mu_A = \mu_B = \mu_C = 1$. ε_C is given by equation (11). Note the five topological states indicated by the arrows. The color scheme is logarithmic. (b) These states correspond to where the imaginary part of the impedance is zero.

from 0. The third closest states to the PBG are seen merging and disappearing with other states in adjacent bands on the far left and far right of the map. As d_C continues to increase, there are temporarily only four states. Therefore in order to have a total of six states, the split topological state must appear after the phase transition.

When the two endlayers are different, we get the sequence *bq...bq*. Figures 2(g)–(i) are *bq*, *bqbq*, and *bqbqbq* respectively. Since there are now an equal number of binary and quaternary crystals in the structure, there is an odd number of interfaces and reversing the order of the components ($bq \rightarrow qb$) will not change the transmission. Figure 2(g) is the familiar single topological state from heterostruture *bq* [34]. For figure 2(h) and (i), the addition of *bq* layers produces resonant states that behave like those discussed previously.

In our second investigation, layer *C* is given a permittivity with frequency dependence, in accordance with the Drude model of dispersion [36],

$$\epsilon_C = 1 - \frac{\xi_p^2}{\xi^2 + ig\xi} \tag{11}$$

where ξ_p and g are the dimensionless plasma and collision frequencies. Equation (11) is plotted in figure 4 with plasma frequency $\xi_p = 2$ and negligible collision frequency $g = 10^{-10}$. Therefore, layer *C* acts as a metal. Layers *A* and *B* remain unchanged. Since the optical path in metal is not constant with frequency, the layer width defined in equations (2) and (3) are given simplier forms,

$$d_A = \frac{\gamma - n_B}{n_A - n_B} - d_C \tag{12}$$

$$d_B = \frac{\gamma - n_A}{n_B - n_A} - d_C. \tag{13}$$

Now, γ is only relevant when defining the layer widths before the metal is introduced. As d_C increases, the band gap closing points are skewed towards higher frequencies due to the behavior of equations (12) and (13). As a concequence of this, topological states in a single interface *bq* system do not start and terminate at the closing points nor are they positioned near the center of the gap. An example of this behavior is shown in figure 5. In figure 5(a), the transmission map is plotted around $\xi = 2$. The metallic layer, d_C, follows the behavior in figure 4. Note that we can have a case where one gap (top center) can support two states. The left state is much sharper than the right one. Also worth noting is that the two center states appear to cross the plasma frequency of the metallic layer without anything unusual happening. This is acceptable because the effective plasma frequency of the entire heterostructure is much lower than the plasma frequency of the metallic inclusion, so the effective permittivity of the heterostructure is positive in the region of these states [41]. This means that all visible gaps in figure 5(a) are classifed as PBGs. There are also two distinct groups of Fabry–Perot resonances. The brighter, more slanted triplets that largely encase the PBGs are caused by coupling among the three interfaces of the four unit cells in the quaternary PC. There is also a fainter vertical triplet of resonances between about $1.72 < \xi < 1.9$, that is caused by the three interfaces in the binary PC. As d_C increases, the leftmost topological state eventually appears to turn into one of these resonances and the rightmost of these states breaks away to become the top-center topological state. The equation $\mathrm{Im}(Z_b + Z_q) = 0$ is plotted in figure 5(b), showing the exact location of those five topological states.

As in the all dielectric case, when there are multiple binary/quaternary interfaces, topological states can split; however, the split states are much closer together, meaning that they are more difficult to resolve [42]. Transmission maps for the *qbq* and *bqb* configurations are displayed in figure 6. While they look very similar to each other and to the single interface system, some subtleties can be pointed out. Resonances in the *qbq* system appear much sharper compared to those in *bqb*. Also the splitting can be seen, although it is more pronounced in *qbq*. Cross sections of the lower center topological state for $d_C = 0.1$ are shown in both structures in figure 7 as the number of interface increases. In figure 7(a), the transmission is shown

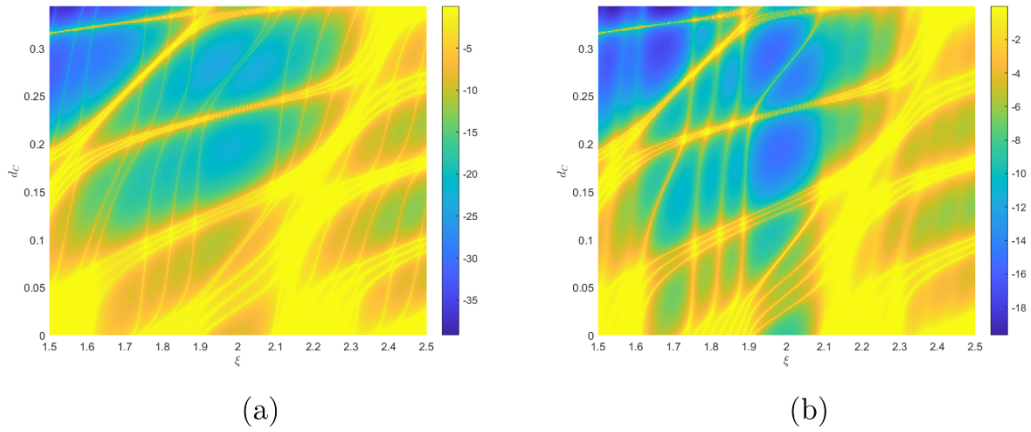

Figure 6. Transmission map for a double interface heterostructure. Layer C of the quaternary PC is frequency dependent. Configuration is (a) *qbq* (b) *bqb*.

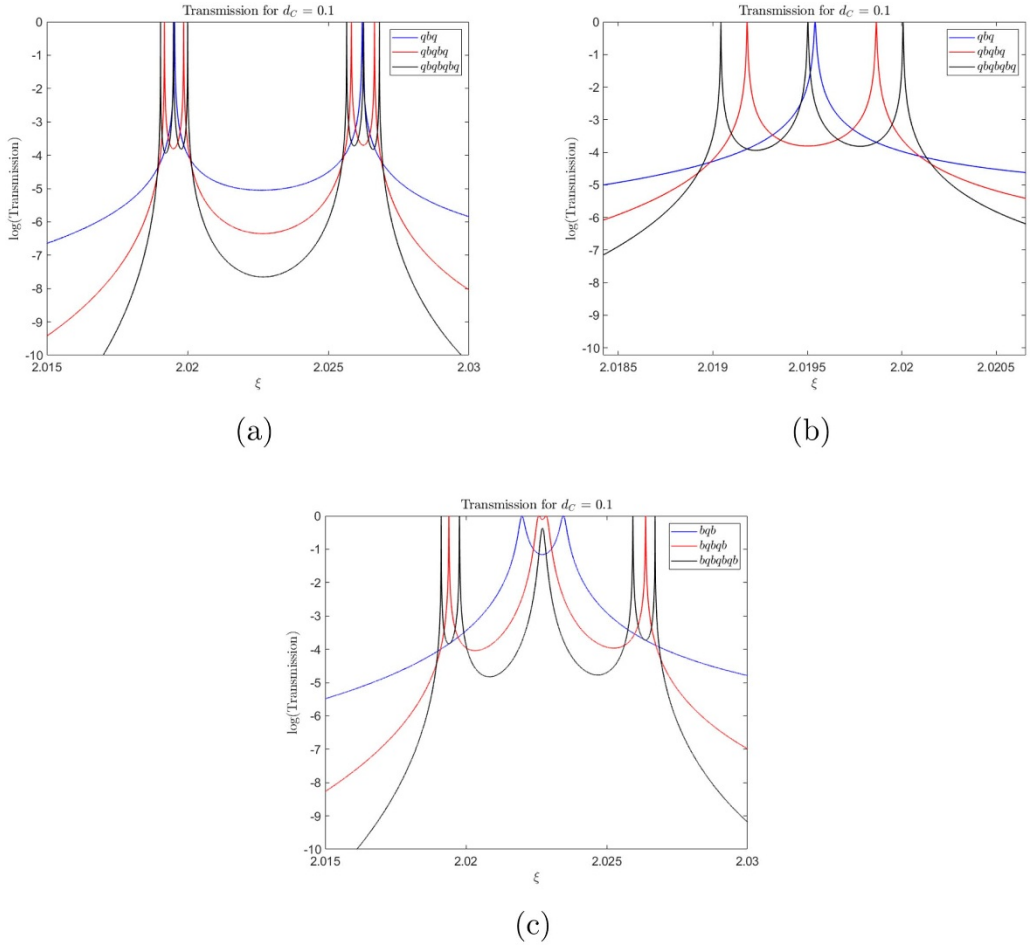

Figure 7. Transmission cross section for the heterostucture in figure 1 with layer C having frequency dependence described by equation (11). All other ε and μ values are the same as in figure 2. (a) Transmission for structures of form *qb...bq*. (b) Zoomed in version of left collection of peaks in (a). (c) Transmission for structures of form *bq...qb*.

for a heterostructure sandwiched between two quaternary PCs. As the number of interfaces increases, each split state itself divides such that the total number equals the number of interfaces. Figure 7(b) zooms into the left cluster of states. If the heterostructure is bounded by binary PCs, shown in figure 7(c), the two central topological split states appear much closer together. As the number of interfaces increases these two eventually merge and the resultant peak decreases. In the plot, this occurs for six interfaces (*bqbqbqb*).This makes it appear that there is a missing state; however, similar to the all dielectric heterostructures *qb...bq* (figures 2(a)–(f)), this merging occurs at lower values of d_C as the number of interfaces increases.

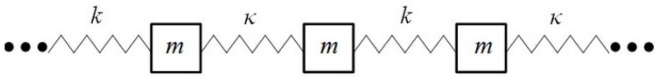

Figure 8. Analogous coupled oscillator model of the heterostructure shown in figure 1. The spring constants represent the PCs and the masses represent interfaces between PCs.

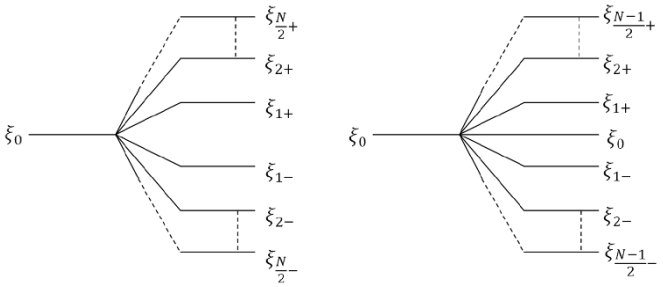

Figure 9. Schematic showing the splitting of the original interface state. The number of interfaces is N. The left diagram represents an even number of interfaces while the right one is for an odd number of interfaces.

Therefore if the transmission cross section was taken for, say, $d_C = 0.08$ rather than for $d_C = 0.1$, then the central peak for structure *bqbqbqb* would instead appear as a small doublet, bringing the total number of states to six.

To help understand what is happening within the heterostructure, it is beneficial to compare the optical system to the more familar 1D coupled harmonic oscillator, shown in figure 8. The interfaces between the individual PCs act as identical masses and the PCs themselves can be thought of as the spring constants [33]. Since there are two different PCs, two distinct spring constants are used. In this example, the constant k corresponds to the binary PC while κ corresponds to the quaternary PC or vice virsa. The topological state will split into a number of states corresponding to the number of interfaces. With an even number of interfaces, the central state vanishes and splits such that half are above the original frequency and half are below. Using this analogy with two interfaces, the lower of the two states is the symmetric state while the higher one is the antisymmetric state [43]. With an odd number of interfaces, the central state still splits as in the even case except now the original state remains. This splitting is shown in figure 9. Overall, the original and split frequencies can be related by an average,

$$\xi_0^2 = \frac{1}{N}\sum_{i=1}^{N}\xi_i^2 \tag{14}$$

where N is the number of PCs in the entire structure and the index, i, is summed through all frequencies after the splitting.

4. Conclusion

We have described the evolution of resonant states in a photonic heterostructure composed of alternating binary and quaternary inversion symmetric photonic crystals as the quaternary crystal transforms from one binary to another. This was done by making the tunable layer in the quaternary crystal a free parameter. Two different heterostructures were given, one in which all components were dielectrics and one in which the free parameter was frequency dependent. For the purely dielectric heterostructure, it was shown that when the structure was sandwiched between two binary PCs, the transmission behavior is similiar to the case of an all binary heterostructure. There is a transmission band of Tamm states, composed in two clusters, in the middle of the PBG, separated by a small gap. When the entire heterostructure is sandwiched by two quaternary PCs, a split topological state appears in this gap, with one fewer Tamm state on either side, as to keep the total number of transmission states equal to the number of interfaces. When the tunable layer in the quaternary PC is frequency dependent, the split topological state appears when the two outermost PCs are binary, rather then quaternary. Unlike for the all dielectric case, a PBG can support more than one transmission group of states, as they no longer start or terminate at the PBG closing points.

While the production of single topological states and their interactions with other states, such as plasmons, has been extremely successful in a wide variety of structures, we believe the heterostructure described in this work provides a novel way for producing a split topological state using just a repeating array of 1D photonic crystals. As stated above, a major disadvantage of this structure is that the splitting is highly dependent on the crystals comprising the end layers. If one PC is incorrect, the state will be single, and if both are incorrect it will vanish, leaving only the surrounding Tamm states. To address this, a possible direction for future research would be to build heterostructures with more complex unit cells. For example, a 6-layer cell could be made inversion symmetric with two tunable layers, allowing for additional parameter spaces to be explored.

ORCID iD

Nicholas J Bianchi https://orcid.org/0000-0003-1708-2826

References

[1] Yablonovitch E 1987 Inhibited spontaneous emission in solid-state physics and electronics *Phys. Rev. Lett.* **58** 2059
[2] John S 1987 Strong localization of photons in certain disordered dielectric superlattices *Phys. Rev. Lett.* **58** 2486
[3] Istrate E, Charbonneau-Lefort M and Sargent E H 2002 Theory of photonic crystal heterostructures *Phys. Rev.* B **66** 075121
[4] Istrate E and Sargent E H 2006 Photonic crystal heterostructures and interfaces *Rev. Mod. Phys.* **78** 455
[5] Tamm I 1932 Über eine mögliche Art der Elektronenbindung an Kristalloberfächen *Z. Phys.* **76** 849
[6] Vinogradov A P, Dorofeenko A V, Erokhin S G, Inoue M, Lisyansky A A, Merzlikin A M and Granovsky A B 2006 Surface state peculiarities in one-dimensional photonic crystal interfaces *Phys. Rev.* B **74** 045128
[7] Vinogradov A P, Dorofeenko A V, Merzlikin A M and Lisyansky A A 2010 Surface states in photonic crystals *Sov. Phys.-Usp* **53** 243

[8] Kavokin A V, Shelykh I A and Malpuech G 2005 Lossless interface modes at the boundary between two periodic dielectric structures *Phys. Rev.* B **72** 233102

[9] Gao D, Mao W, Zhang R, Liu J, Zhao Q, Tam W Y and Wang X 2019 Tunable interface state in one dimensional composite photonic structure *Opt. Comm* **453** 124324

[10] Lin L L and Li Z Y 2001 Interface states in photonic crystal heterostructures *Phys. Rev.* B **63** 033310

[11] Feng S, Sang H Y, Li Z Y, Cheng B Y and Zhang D Z 2005 Sensitivity of surface states to the stack sequence of one-dimensional photonic crystals *J. Opt. A: Pure Appl. Opt.* **7** 374

[12] Zheng Y, Wang Y, Lou J and Xu P 2018 Optical Tamm states in photonic structures made of inhomogeneous material *Opt. Comm* **406** 103

[13] El Abouti O, El Boudouti E H, El Hassouani Y, Noual A and Djafari-Rouhani B 2016 Optical Tamm states in one-dimensional superconducting photonic crystal *Phys. Plasmas* **23** 082115

[14] Wang T B, Yin C P, Liang W Y, Dong J W and Wang H Z 2009 Electromagnetic surface modes in one-dimensional photonic crystals with dispersive metamaterials *J. Opt. Soc. Am.* B **26** 1635

[15] Barvestani J, Kalafi M, Soltani-Vala A and Namdar A 2008 Backward surface electromagnetic waves in semi-infinite one-dimensional photonic crystals containing left-handed materials *Phys. Rev.* A **77** 013805

[16] Namdar A, Shadrivov I V and Kivshar Y S 2006 Backward Tamm states in left-handed metamaterials *Appl. Phys. Lett.* **89** 114104

[17] Hajian H, Rezaei B, Vala A S and Kalafi M 2012 Tuned switching of surface waves by a liquid crystal cap layer in one-dimensional photonic crystals *Appl. Opt.* **51** 2909

[18] Bashiri J, Rezael B, Barvestani J and Zapata-Rodriguez C J 2019 Bloch surface waves engineering in one-dimensional photonic crystals with a chiral cap layer *J. Opt. Soc. Am.* B **36** 2106

[19] Kaliteevski M, Iorsh I, Brand S, Abram R A, Chamberlain J M, Kavokin A V and Shelykh I A 2007 Tamm plasmon-polaritons: possible electromagnetic states at the interface of a metal and a dielectric Bragg mirror *Phys. Rev.* B **76** 165415

[20] Brand S, Kaliteevski M A and Abram R A 2009 Optical Tamm states above the bulk plasma frequency at a Bragg stack/metal interface *Phys. Rev.* B **79** 085416

[21] Zhou H, Yang G, Wang K, Long H and Lu P 2010 Multiple optical Tamm states at a metal-dielectric mirror interface *Opt. Lett* **35** 4112

[22] Xiao M, Zhang Z Q and Chan C T 2014 Surface impedance and bulk band geometric phases in one-dimensional systems *Phys. Rev.* X **4** 021017

[23] Zak J 1989 Berry's phase for energy bands in solids *Phys. Rev. Lett.* **62** 2747

[24] Choi K H, Ling C W, Lee K F, Tsang Y H and Fung K H 2016 Simultaneous multi-frequency topological edge modes between one-dimensional photonic crystals *Opt. Lett.* **41** 1644

[25] Wang L, Cai W, Bie M, Zhang X and Xu J 2018 Zak phase and topological plasmonic Tamm states in one-dimensional plasmonic crystals *Opt. Express* **26** 28963

[26] Yang Y, Xu T, Xu Y F and Hang Z H 2017 Zak phase induced multiband waveguide by two dimensional photonic crystals *Opt. Lett.* **42** 3085

[27] Tolmachev V A 2017 Optical properties of one-dimensional photonic crystals obtained by micromatchining silicon (a review) *Opt. Spectrosc.* **122** 646

[28] Tolmachev V A, Baldycheva A V, Krutkova E Y, Perova T S and Berwick K 2009 Optical characteristics of a one-dimensional photonic crystal with an additional regular layer *Proc. SPIE* **7390** 739017

[29] Baldycheva A V, Tolmachev V A, Perova T S and Berwick K 2010 Design of three-component one-dimensional photonic crystals for alteration of optical contrast and omni-directional reflection *Proc. SPIE* **7713** 771321

[30] Zhang W L, Jiang Y, Zhu Y Y, Wang F and Rao Y J 2013 All-optical bistable logic control based on coupled Tamm plasmons *Opt. Lett.* **38** 4092

[31] Wang X, Liang Y, Wu L, Guo J, Dai X and Xiang Y 2018 Multi-channel perfect absorber based on a one-dimensional topological photonic crystal heterostructure with graphene *Opt. Lett.* **43** 4256

[32] Hu J, Yao E, Xie W, Liu W, Li D, Lu Y and Zhan Q 2019 Strong longitudinal coupling of Tamm plasmon polaritons in graphene/DBR/Ag hybrid structure *Opt. Express.* **27** 18642

[33] Hu J, Liu W, Xie W, Zhang W, Yao E, Zhang Y and Zhan Q 2019 Strong coupling of optical interface modes in a 1D topological photonic crystal heterostructure/Ag hybrid system *Opt. Lett.* **44** 5642

[34] Bianchi N and Kahn L 2020 Topological photonic states at a 1D binary-quaternary interface arXiv:1910.02920

[35] Chen Z, Han P, Leung C W, Wang Y, Hu M and Chen Y 2012 Study of optical Tamm states based on the phase properties of one-dimensional photonic crystals *Opt. Express* **20** 21618

[36] Jackson J D 1999 *Classical Electrodynamics* (New York: Wiley)

[37] Yariv A and Yeh P 1984 *Optical Waves in Crystals: Propagation and Control of Laser Radiation* (New York: Wiley)

[38] Orfanidis S J 2016 *Electromagnetic Waves and Antennas* (Newark, Camden: Rutgers University)

[39] Durach M and Rusina A 2012 Transforming Fabry–Perot resonaces into a Tamm mode *Phys. Rev.* B **86** 235312

[40] Xiao-Qin H and Yi-Ping C 2003 Degeneracy and split of defect states in photonic crystals *Chin. Phys. Lett.* **20** 1721

[41] Manzanares-Martinez J 2010 Analytic expression for the effective plasma frequency in one-dimensoinal metallic-dielectric photonic crystal *Prog. Electromagn. Res.* M **13** 189

[42] Markos P and Soukoulis C M 2008 *Wave Propagation: From Electrons to Photonic Crystals and Left-Handed Materials* (Princeton, NJ: Princeton University)

[43] Thornton S T and Marion J B 2008 *Classical Dynamics of Particles and Systems* (Boston, MA: Cengage Learning)